Nanoscale

Accepted Manuscript

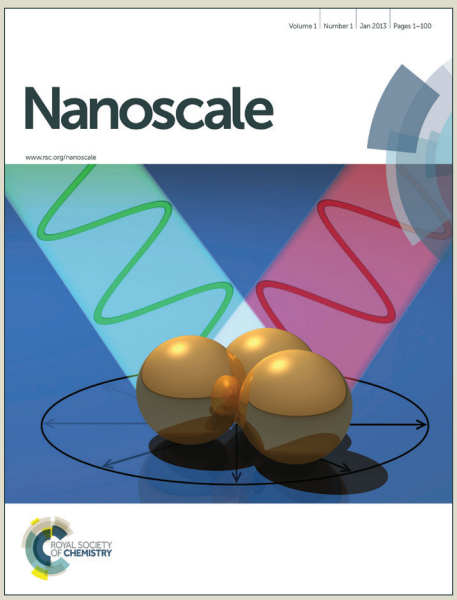

This is an *Accepted Manuscript*, which has been through the Royal Society of Chemistry peer review process and has been accepted for publication.

Accepted Manuscripts are published online shortly after acceptance, before technical editing, formatting and proof reading. Using this free service, authors can make their results available to the community, in citable form, before we publish the edited article. We will replace this *Accepted Manuscript* with the edited and formatted *Advance Article* as soon as it is available.

You can find more information about *Accepted Manuscripts* in the Information for Authors.

Please note that technical editing may introduce minor changes to the text and/or graphics, which may alter content. The journal's standard Terms & Conditions and the Ethical guidelines still apply. In no event shall the Royal Society of Chemistry be held responsible for any errors or omissions in this *Accepted Manuscript* or any consequences arising from the use of any information it contains.

ROYAL SOCIETY OF CHEMISTRY

www.rsc.org/nanoscale

Journal Name

RSCPublishing

ARTICLE

Pentacene on Ni(111): room-temperature molecular packing and temperature-activated conversion to graphene†

L. E. Dinca,[a] F. De Marchi,[a] J. M. MacLeod,[a,*] J. Lipton-Duffin,[a] R. Gatti,[a] D. Ma,[a] D. F. Perepichka[b,c] and F. Rosei[a,c,*],

Cite this: DOI: 10.1039/xoxxoooooox

Received ooth January 2012,
Accepted ooth January 2012

DOI: 10.1039/xoxxoooooox

www.rsc.org/

We investigate, by using scanning tunnelling microscopy, the adsorption of pentacene on Ni(111) at room temperature and the behaviour of these monolayer films with annealing up to 700 °C. We observe the conversion of pentacene into graphene, which begins from as low as 220 °C with the coalescence of pentacene molecules into large planar aggregates. Then, by annealing at 350 °C for 20 minutes, these aggregates expand into irregular domains of graphene tens of nanometers in size. On surfaces where graphene and nickel carbide coexist, pentacene shows preferential adsorption on the nickel carbide phase. The same pentacene to graphene transformation was also achieved on Cu(111), but at a higher activation temperature, producing large graphene domains that exhibit a range of moiré superlattice periodicities.

INTRODUCTION

Conversion of polycyclic aromatic molecules to graphene has recently gained attention,[1-4] as it may provide an easy route to synthesizing one of the most remarkable systems of recent years.[5] The growth of graphene has been carried out using various organic precursors,[1, 2, 6] at temperatures ranging from 300 to 1000 °C. A recent report shows the feasibility of low temperature nickel-promoted synthesis of graphene multilayers on non-conductive surfaces, such as plastic or glass.[7] On Ni(111) (Table 1), the growth of graphene is of special interest due to the very close lattice match between the two materials, allowing the formation of a 1×1 overlayer structure,[8] and hybridization between the graphene π-states and the nickel d-band and shallow surface states.[9] These interaction channels induce the strong adsorption of graphene on Ni(111) as compared to other metallic surfaces:[10] the graphene-nickel substrate separation is up to 0.12 nm shorter than for bulk graphite (0.335 nm),[11] while on Cu(111) this reduction is only 0.05 nm.[12] This strong interaction modifies the electronic structure of the graphene overlayer on Ni(111), as compared to free standing graphene, and leads to very interesting electronic (band-gap opening),[10] and magnetic effects.[13] Graphene overlayers can also provide new opportunities for the growth of self-assembled architectures by tailoring the surface reactivity of the supporting metallic surfaces,[14] motivating thereby the study of molecules at graphene interfaces.[15, 16]

Surface	Precursor	T [°C]	Quality-check/Ref.
Ni(111)	CO	> 300	ILS, ELS,[17]
	Ethylene (C_2H_4)	475	Auger,[18]
	Propylene(C_3H_6)	500	[19-24]
	Ethylene (C_2H_4)	400-500	STM,[25]
	Ethylene (C_2H_4)	425-525	STM,[26]
	Ethylene (C_2H_4)	~550	LEEM,[27]
	Toluene (C_7H_8)	400-650	STM,[28, 29]
	Ethylene (C_2H_4)	460-650	STM, Auger,[30, 31]
	Ethylene (C_2H_4)	675	STM,[13]
Ni(111)/ W(110)	Propylene(C_3H_6)	400	ARPES,[32]
Ni(111)/ MgO(111)	Propylene(C_3H_6)	600-680	STM, LEEM,[33]
Ni/SiO_2	Graphite powder	25-260	Raman,[7]
Ni/plastic /glass	Graphite powder	< 160	Raman,[7]

Table 1 Graphene growth on Ni(111) as well as plastic/glass surfaces coated with a Ni film (the Ni films in Ref. 7 had a strong (111) texture);[7] reported precursors and thermal conditions. Results from extended temperature, up to 1000 °C, are presented in the Table S1, ESI. (ILS – ionization loss spectroscopy, ELS – energy-loss spectroscopy, LEED – low-energy electron diffraction, STM – scanning tunnelling microscopy, LEEM – micro LEED, ARPES – angle-resolved photoemission spectroscopy.)

Pentacene ($C_{22}H_{14}$) is a polycyclic aromatic hydrocarbon containing 5 benzene rings. It has been widely studied in three-dimensional crystals,[34] and in two-dimensional (2D) films on surfaces,[35, 36] because of its relatively high carrier mobility and consequently good performance as a semiconductor in organic electronic devices. In essence, pentacene can be considered as a

Nanoscale Accepted Manuscript

structural element of graphene. Conversion of pentacene to graphene by covalent C─C coupling between pentacene molecules requires C─H bond breaking and subsequent rebonding of the undercoordinated carbon atoms.[2] Unlike coronene,[37] whose symmetry matches the final symmetry of graphene, pentacene has a lower symmetry. This symmetry reduction may make pentacene a good candidate for growing novel graphene nanoarchitectures, such as *e.g.* ribbons,[38] under suitable synthetic conditions.

We studied the adsorption of pentacene on Ni(111) by means of scanning tunnelling microscopy (STM). The temperature-activated conversion of pentacene to graphene and the subsequent adsorption of pentacene on the newly formed graphene layer were explored. The same pentacene to graphene conversion was conducted on Cu(111) films,[39] and a comparison of the growth process on these two surfaces is presented.

Experimental section

All experiments were carried out under ultrahigh vacuum (UHV) conditions in a chamber with a base pressure of 10^{-10} mbar. The Ni(111) substrate was cleaned by repeated cycles of sputtering with 1 keV Ar^+ for 15 minutes followed by annealing at 850 °C for 20 minutes.[40]

Epitaxial Cu(111) films of 50-100 nm thick were grown on Al_2O_3 (0001) crystals using a method similar to the one described by Katz.[41] To achieve good quality Cu films the substrate was held at 250-300 °C,[42] while the Cu deposition rate was maintained at ~0.01 nm/s.

Pentacene (98% purity, ACROS Organics) was sublimated from a Knudsen-type effusion cell with pyrolitic boron nitride or Al_2O_3 crucibles, held at approximately 190 °C. During deposition the substrates were held at room temperature (RT). After deposition and characterization of the RT pentacene layer, the samples were annealed at specific temperatures for times varying from 15 min. to 3 hours. The temperatures are estimated to be accurate within ±25 °C.

STM characterization was performed at RT using a commercial variable-temperature instrument (Aarhus 150, SPECS GmbH) equipped with cut Pt/Ir tips. Bias voltages are reported with respect to the STM tip. To compensate for instrumental drift and creep, the STM images were corrected to reflect known dimensions of experimental features wherever possible, and flattened, smoothed or Fourier filtered to enhance salient details by using the WSxM software.[43] The STM images in this work contain results representative of much larger data sets.

Computational studies were performed within the density functional theory (DFT) formalism, based on the local density approximation (LDA). Pseudopotentials constructed with modified Troullier-Martins (TM) scheme,[44] and the Perdew-Zunger (PZ) exchange-correlation energy functional (successfully used for aromatics as coronene)[45] implemented in the SIESTA software package, were employed.[46-48] To model the adsorption of pentacene on Ni(111), a single pentacene molecule was considered on the Ni surface. The minimum-energy of the pentacene/Ni(111) was determined by investigating different possible adsorption sites with various pentacene-substrate orientations. In all the calculations, an optimum kinetic energy cutoff (from single point calculations) of 240 Ry was used for the plane wave expansion. The Ni(111) surface was modelled with a 2D slab in a periodic 6×8 cell with the inclusion of a vacuum (~1.5 nm) layer to avoid interaction between the slabs. For this metallic system, a three layer slab was found to be sufficiently large to represent (and converge) the Ni(111) surface structure. All the geometry optimizations took the nickel magnetization into account by considering the spin polarization, and employing an algorithm based on the conjugate gradient method.[49] During simulations, the top layer of the nickel surface was allowed to relax, whereas the atoms in all remaining layers were kept fixed in their bulk-like positions. The optimized shapes of precursor molecular structures result from gas phase DFT calculations by using Gaussian 09 at the B3LYP/6-31G(d) level.[50] Avogadro,[51] and free Discovery Studio Visualization,[52] open-source molecular builders and visualization tools were used for producing basic molecular models.

Results and discussion

Ni(111) surface

Following RT deposition onto Ni(111), pentacene molecules pack into a "random tiling" phase, as shown in Fig. 1 and Fig. 2(a) and (c). In this phase, which was also observed on Cu(111),[36] the pentacene molecules are aligned along the $\langle 1\bar{1}0 \rangle$ directions; since the directional alignment of any one molecule cannot be inferred from the directional alignment of its neighbours, the phase is referred to as "random". Our investigation reported in detail in Fig. 2 revealed a slight preference for pentacene adsorbed in the vicinity of terrace edges to align with its long axis parallel to the steps. However, away from steps, this preferential adsorption was lost, and the molecules oriented randomly (Fig. 2(e),(f)).

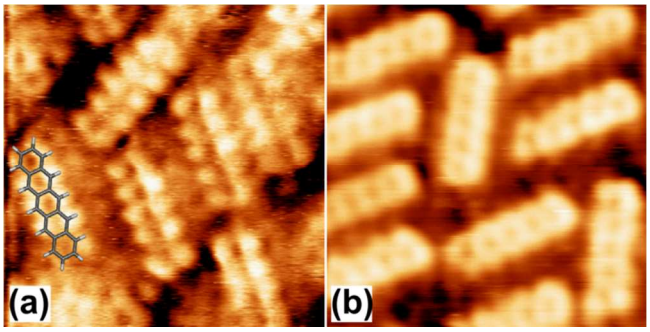

Fig. 1 3×3 nm^2 STM images of pentacene molecules adsorbed on a Ni(111) substrate at RT. (1.49 nA and 1.8 mV for (a); 0.53 nA and 31.1 mV for (b)). A molecular model was superimposed in (a).

Unlike the random tiling phase observed on Cu(111),[36] where the apparent lengths of pentacene molecules are not equivalent, due to oscillations between adsorption sites, in the Ni-supported

Nanoscale Accepted Manuscript

This journal is © The Royal Society of Chemistry 2012

phase all the pentacene molecules have equal apparent length indicating that the molecules are strongly adsorbed to the surface (see also Fig. S1, Fig. S2, ESI).

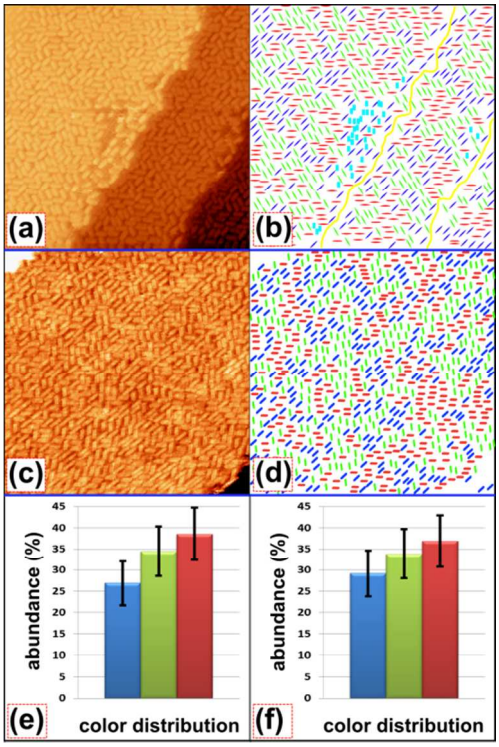

Fig. 2 Quantitative analysis of pentacene orientation on Ni(111). STM image of pentacene as-deposited on Ni(111) surface centred on a step abundant region is presented in (a) and away from the stepped region in (c). Both images are 30×30 nm^2. Scanning parameters: 1.36 nA, 1.8 mV for (a); 2.05 nA and 2.5 mV for (c). A statistical analysis of pentacene distribution in images (a) and (c) is presented in the color-coded images (b) and (d) respectively, with blue, green and red lines representing the pentacene molecules and, each colour type corresponding to orientation along one of the $\langle 1\bar{1}0 \rangle$ directions; long yellow lines depict the lines of the step edges, while in (b) the cyan scattered spots represent the nickel-carbide structures. The quantitative representation of the molecular abundance, related to the specific colours of (b) and (d) is plotted in (e) and (f) respectively. The numerical values in the error bars were calculated as the standard deviation assuming Poisson statistics.

To assign a model to the random tiling phase, we investigated six possible adsorption geometries using DFT. An isolated pentacene molecule finds its minimum energy in one of the "*hollow-fcc*" or "*bridge-top*" positions (the variation in binding energy is less than 0.06 eV), as shown in Fig. S3(d) and (e) respectively (from ESI).

Annealing leads to the coalescence of the pentacene molecules, and converts the uniformly distributed monolayer of individual molecules into small domains of graphene. The process starts at 220 °C (Fig. S4, from ESI), and the domain size improves by annealing at 250 and 350 °C for 30 and 20 minutes respectively, as shown in Fig. 3(a) and (c). High-resolution imaging of these domains reveals hexagonal features (Fig. 3(b) and (d)), with a measured periodicity of 0.24±0.05 nm, consistent with both the in-plane lattice constant of graphite (0.246 nm) and the lattice constant for the (111) surface of nickel (0.249 nm).[53] The epitaxial growth of graphene on Ni(111) has been widely studied, and graphene was shown to grow in two distinct geometries:[54] the *top-fcc*, with one carbon atom adsorbed at the on-top position and the other on the *hollow-fcc* site, and *bridge-top* position, with two carbon atoms equivalently positioned and shifted off-centre above one Ni atom. The geometries for these phases are similar to the ones presented for single pentacene molecule adsorbed on the Ni(111) surface, in Fig. S3(d) and (e), respectively (see ESI).

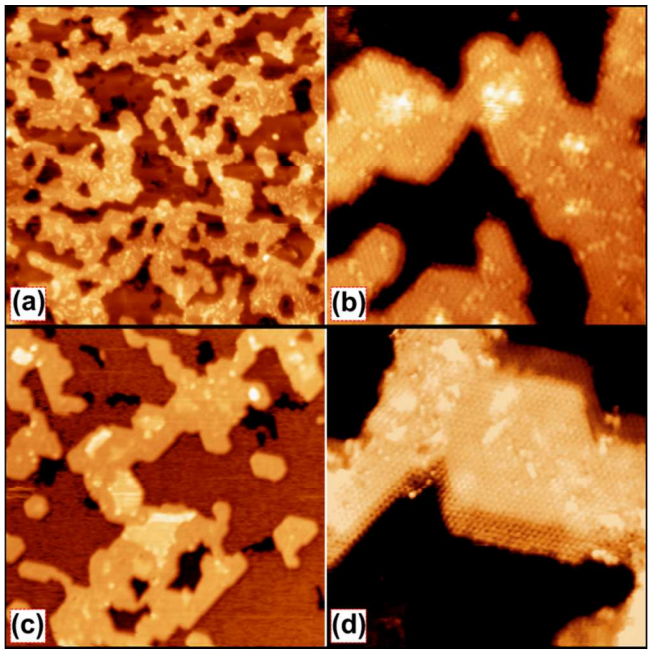

Fig. 3 STM images of graphitic domains on Ni(111). Prior to imaging, the samples were annealed for 30 minutes at 250 °C in (a) and (b), and for 20 minutes at 350 °C in (c) and (d). STM parameters: 50×50 nm^2, 1.77 nA, 4.6 mV in (a); 10×10 nm^2, -5.28 nA, -1.2 mV in (b); 50×50 nm^2, 0.65 nA, 3.4 mV in (c); 10×10 nm^2, -1.52 nA, and -19.5 mV in (d).

We attribute the graphene formation to dehydrogenation of the pentacene precursor,[2] and subsequent intermolecular rebonding with molecular diffusion occurring at one or more points in the process. In a number of recent reports, this strategy of C─H bond activation has been demonstrated to be effective for on-surface polymerization.[38, 55-58] Partial dehydrogenation of pentacene leading to peripentacene and related C–C coupled products has also been suggested to occur during high-temperature vacuum sublimation in an inert gas flow (350 °C),[59] and likely attributable to catalytic impurities in the sample. In our case, using Ni(111) both as a catalyst and support, the activation temperature was reduced to roughly 220 °C.

The structural order of the graphene domains improves by increasing the annealing temperature, as shown in Fig. 3. However, the graphene growth is patchy and incomplete, which can be attributed to compacting after hydrogen removal. Although this suggests nearly complete hydrogen removal, some hydrogen is likely retained at domain boundaries and defects. The morphology depends on the annealing temperature as well as on the initial coverage of pentacene. At a similar activation temperatures, a pentacene coverage below 1

Nanoscale Accepted Manuscript

monolayer (<ML) produces graphene with a low defect density and large domains (up to 650 nm^2), which could be due to the fact that all molecules experience catalytic interaction with the substrate (Fig. 3). At >ML pentacene coverage, annealing temperatures near 600 °C produced large domains of high-quality graphene, whereas annealing below 400 °C produced domains with poor internal quality (Fig. S5, ESI).

DFT calculations[60, 61] and various experimental reports suggest that the step edges are more reactive in dissociating small diatomic molecules such as CO, NO, O_2 and N_2.[61] Experiments at room temperature involving ethylene on Ni(111) show a more pronounced reactivity towards the breaking of carbon-carbon bonds than carbon-hydrogen bonds at step edges,[62] suggesting that the flat (111) facets may therefore play an important role in dehydrogenation. As a consequence of carbon-carbon bond dissociation, carbidic domains localized at the step edges can form on the Ni(111) surface at temperatures as low as 200 °C.[26] Monolayer graphene growth from large aromatic precursors should be thermodynamically favoured with respect to the nickel carbide (Ni_2C) surface phase on Ni(111), although the latter may be promoted at low carbon density.[31]

In our experiments, nickel carbide, which was identified by its known $\sqrt{39}\,\overline{R}16.1° \times \sqrt{39}R16.1°$ reconstruction,[17, 26] formed at step edges on surfaces annealed to 700 °C for 20 minutes (see Fig. S6, ESI). In general, it is difficult to create mixed carbide and graphene domains above 600 °C due to the continuous consumption of the carbide structure by the advancing graphene front.[63] Their coexistence following higher annealing temperatures in the present experiments may be explained by the relatively short annealing times used.

By depositing pentacene onto graphene/Ni(111) surfaces on which Ni_2C coexists with graphene, held at RT, we were able to compare the relative adsorption properties of these two phases (Fig. 4; and Fig. S6, ESI).[29] The single molecules adsorbed preferentially on the Ni_2C, implying their stronger interaction with the nickel carbide than with graphene, consistent with the relatively low adsorption energies reported for graphene.[15, 62]

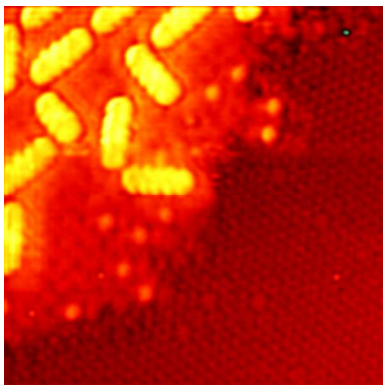

Fig. 4 7×7 nm^2 STM image of pentacene on a Ni(111) surface with coexisting domains of nickel carbide (left upper side) and graphene (right lower side). Scanning parameters: 0.97 nA, 3.4 mV.

Raman spectroscopy is widely used in the characterization of the strain and defects present in graphene layers.[64] However, for the particular case of monolayer graphene on Ni(111), the Raman signal is suppressed due to the strong graphene-nickel interaction.[10] Hybridization of the nickel *d*-electrons with π-electrons of graphene induces a down shift in the π bands, opening a gap in the electronic structure of graphene and therefore annihilating the electron-phonon coupling essential for a detectable vibrational effect by Raman spectroscopy. Accordingly, we did not observe any Raman response in our graphene/Ni(111).[65]

Similarly, although using scanning tunnelling spectroscopy (STS) to probe the local density of states (LDOS) can produce characteristic spectra for graphene that interacts only weakly with its support,[66] the interpretation becomes more difficult in graphene grown on Ni(111). In published STS data from graphene on Ni(111), "signature" graphene features are missing, and the spectra instead appear qualitatively similar to those obtained prior to graphene growth on the Ni(111).[67] Furthermore, the nanoscale dimensions of the graphene could introduce additional perturbations to its electronic structure, as it is known to do in the case of nanoribbons.[38, 68]

Cu(111) surface

We also investigated the process of pentacene conversion to graphene on Cu(111), as a control experiment.[41, 69] At low pentacene coverage (<0.25 ML) and RT, the pentacene molecules diffuse freely on the surface. Upon annealing above 350 °C, the molecules merge into branched nanoribbon structures, likely due to partial dehydrogenation and subsequent oligomerization (Fig. 5).

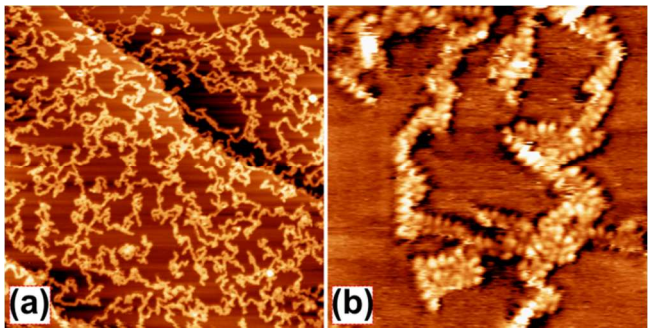

Fig. 5 Spaghetti like structures obtained from pentacene deposited on Cu(111) after annealing for 30 minutes at ~350 °C (70×70 nm^2, 0.5 nA, 1250 mV for (a), and 6×6 nm^2, -1.7 nA, -45 mV for (b)).

Starting from a full pentacene monolayer on Cu(111), graphene domains tens of nanometers in size were obtained only above 800 °C (as shown in Fig. 6(a)). Characteristic moiré patterns exhibit continuously varying orientations and periodicities.[70, 71] Graphene grown by CVD on copper substrates has previously been shown to exhibit a high proportion of small-angle domain boundaries.[72] Our analysis of the moiré patterns from the left and right of the image in Fig. 6 indicates that the graphene lattices in these regions are rotated by 2° with respect to one another (Fig. 6(b)). However, we cannot reproduce the

Nanoscale Accepted Manuscript

This journal is © The Royal Society of Chemistry 2012

continuous moiré pattern by using a single domain boundary between the two sheets of graphene, suggesting instead that multiple low-angle domain boundaries must coexist across the region denoted by the black solid line in (b).

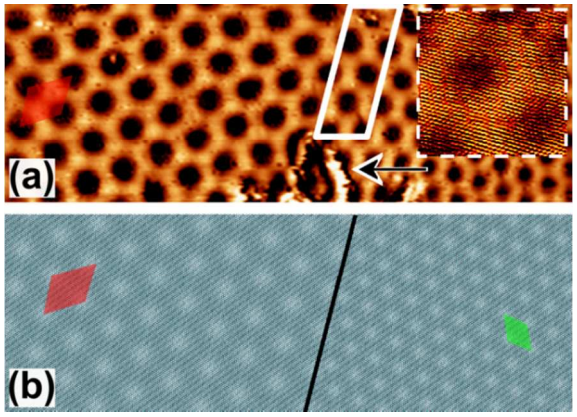

Fig. 6 69×24 nm^2 STM image of graphene on Cu(111) in (a), obtained from pentacene precursor at temperature ~800 °C (and annealing for 15 minutes). Imaging parameters: 4.32 nA and 38 mV. Atomic resolution inside the moiré pattern is presented in the inset image (6.5×6.5 nm^2). Two moiré domains, rotated by roughly 40° with respect to each other, are represented by their resolved unit cells, indicated by the red and green rectangles. The measured periodicity, for each moiré domain, is 4.9±0.2 nm (red unit cell) and 3.3±0.2 nm respectively (green unit cell).[71, 73] The transition between the two moiré patterns occurs uniformly over several nanometers (framed by the white rectangle). A model of image (a) is presented in (b), generated by rotating two graphene sheets, anticlockwise by 2° (left) and 4° (right), with respect to the Cu(111) substrate, to obtain separate domains of moiré patterns, with inside periodicities matching the experimental values. The 0° position is defined for the armchair of graphene aligned along the close-packed ⟨1$\bar{1}$0⟩ directions of Cu(111).

Conclusions

In conclusion, we investigated the structure and temperature dependence of pentacene monolayers on Ni(111). As-deposited on Ni(111), the pentacene forms a dense monolayer with flat-lying molecules oriented along the ⟨1$\bar{1}$0⟩ directions. Upon annealing above 220 °C, it converts into small domains of graphene, tens of nanometers in size, at temperatures lower than those previously documented (Table 1). Improved graphene quality was obtained by annealing at temperatures up to 700 °C. Comparison of molecular adsorption on graphene and adjacent nickel carbide domain demonstrates that at RT pentacene preferentially adsorbs on the nickel carbide. The pentacene to graphene conversion occurs on Cu(111) only at temperatures above 800 °C. While we hope to continue to refine and characterize the graphene produced from pentacene on Ni(111), we also plan the extension of this technique to Ni(111) films on α-Al_2O_3,[74] polycrystalline nickel surface, or adapt it to non-UHV conditions as well. However, although previous work has suggested that it may be difficult to produce uniform graphene growth on surfaces such as alpha-Al_2O_3,[74] the nickel films can then be dissolved, allowing us to harvest the graphene for subsequent characterization via Raman spectroscopy, without the influence of the Ni(111) substrate.

Acknowledgements

This work was supported by the Natural Sciences and Engineering Research Council of Canada (NSERC) through Discovery Grants (D.F.P., D.M. and F.R.), as well as the Fonds de Recherche du Québec – Nature et Technologies (FRQNT) through a Team Grant and the Ministère du Développement Economique, de l'Innovation et de l'Exportation (MDEIE) through an international collaboration Grant. F.R. is grateful to the Canada Research Chairs program for partial salary support and is grateful to the Alexander von Humboldt Foundation for a F.W. Bessel Award. F.R. also acknowledges NSERC for an EWR Steacie Memorial Fellowship and Elsevier for a grant from Applied Surface Science. L.E.D. acknowledges a graduate fellowship from FRQNT. L.E.D. thanks Group NanoXplore Inc. for helpful discussions, Luis Cardenas for helping with Raman experiments and Csaba E. Szakacs for guidance regarding the DFT calculations. This research has been enabled by the use of computing resources provided by Compute/Calcul Canada.

Notes and references

[a] Centre Énergie, Matériaux et Télécommunications, Institut National de la Recherche Scientifique, Université du Québec, 1650 boulevard Lionel-Boulet, Varennes, QC, J3X 1S2, Canada.
[b] Department of Chemistry, McGill University, 801 Sherbrooke Street West, Montreal, QC, H3A 0B8, Canada.
[c] Center for Self-Assembled Chemical Structures, McGill University, 801 Sherbrooke Street West, Montreal, QC, H3A 0B8, Canada.
* Correspondence should be addressed to: macleod@emt.inrs.ca; rosei@emt.inrs.ca.

† Electronic Supplementary Information (ESI) available: Summary of used growth methods for graphene/Ni(111), STM images of pentacene/Ni(111), graphitic structures on Ni(111), pentacene adsorbed on carbide, DFT calculations of pentacene/Ni(111) ─ the adsorption sites. See DOI: 10.1039/b000000x/

1. L. Chen, Y. Hernandez, X. Feng and K. Müllen, *Angew. Chem., Int. Ed.*, 2012, **51**, 7640.
2. X. Wan, K. Chen, D. Liu, J. Chen, Q. Miao and J. Xu, *Chem. Mater.*, 2012, **24**, 3906.
3. A.-F. Tran-Van and H. Wegner, Springer Berlin Heidelberg, 2013, ch. 465, p. 37.
4. Y. Ishii, H. Y. Song, H. Kato, M. Takatori and S. Kawasaki, *Nanoscale*, 2012, **4**, 6553.
5. A. K. Geim and K. S. Novoselov, *Nat. Mater.*, 2007, **6**, 183.
6. M. Batzill, *Surf. Sci. Rep.*, 2012, **67**, 83.
7. J. Kwak, J. H. Chu, J.-K. Choi, S.-D. Park, H. Go, S. Y. Kim, K. Park, S.-D. Kim, Y.-W. Kim, E. Yoon, S. Kodambaka and S.-Y. Kwon, *Nat. Commun.*, 2012, **3**, 645.
8. J. Wintterlin and M. L. Bocquet, *Surf. Sci.*, 2009, **603**, 1841.
9. J. Lobo-Checa, T. Okuda, M. Hengsberger, L. Patthey, T. Greber, P. Blaha and J. Osterwalder, *Phys. Rev. B*, 2008, **77**, 075415.
10. A. Dahal and M. Batzill, *Nanoscale*, 2014, **6**, 2548.
11. Y. Gamo, A. Nagashima, M. Wakabayashi, M. Terai and C. Oshima, *Surf. Sci.*, 1997, **374**, 61.

Nanoscale Accepted Manuscript

12. G. Giovannetti, P. A. Khomyakov, G. Brocks, V. M. Karpan, J. van den Brink and P. J. Kelly, *Phys. Rev. Lett.*, 2008, **101**, 026803.
13. L. V. Dzemiantsova, M. Karolak, F. Lofink, A. Kubetzka, B. Sachs, K. von Bergmann, S. Hankemeier, T. O. Wehling, R. Fromter, H. P. Oepen, A. I. Lichtenstein and R. Wiesendanger, *Phys. Rev. B*, 2011, **84**, 205431.
14. L. Massimi, S. Lisi, D. Pacile, C. Mariani and M. G. Betti, *Beilstein J. Nanotechnol.*, 2014, **5**, 308.
15. J. M. MacLeod and F. Rosei, *Small*, 2014, **10**, 1038.
16. A. J. Martínez-Galera, N. Nicoara, J. I. Martínez, Y. J. Dappe, J. Ortega and J. M. Gómez-Rodríguez, *J. Phys. Chem. C*, 2014, **118**, 12782.
17. R. Rosei, S. Modesti, F. Sette, C. Quaresima, A. Savoia and P. Perfetti, *Phys. Rev. B*, 1984, **29**, 3417.
18. A. Cupolillo, N. Ligato and L. S. Caputi, *Carbon*, 2012, **50**, 2588.
19. W. D. Dou, S. P. Huang, R. Q. Zhang and C. S. Lee, *J. Chem. Phys.*, 2011, **134**, 094705.
20. A. M. Shikin, G. V. Prudnikova, V. K. Adamchuk, F. Moresco and K. H. Rieder, *Phys. Rev. B*, 2000, **62**, 13202.
21. D. Marchenko, A. Varykhalov, A. Rybkin, A. M. Shikin and O. Rader, *Appl. Phys. Lett.*, 2011, **98**, 122111.
22. A. M. Shikin, V. K. Adamchuk and K. H. Rieder, *Phys. Solid State*, 2009, **51**, 2390.
23. Y. S. Dedkov, A. M. Shikin, V. K. Adamchuk, S. L. Molodtsov, C. Laubschat, A. Bauer and G. Kaindl, *Phys. Rev. B*, 2001, **64**, 035405.
24. M. Weser, Y. Rehder, K. Horn, M. Sicot, M. Fonin, A. B. Preobrajenski, E. N. Voloshina, E. Goering and Y. S. Dedkov, *Appl. Phys. Lett.*, 2010, **96**, 012504.
25. F. Bianchini, L. L. Patera, M. Peressi, C. Africh and G. Comelli, *J. Phys. Chem. Lett.*, 2014, **5**, 467.
26. C. Klink, I. Stensgaard, F. Besenbacher and E. Laegsgaard, *Surf. Sci.*, 1995, **342**, 250.
27. R. Addou, A. Dahal, P. Sutter and M. Batzill, *Appl. Phys. Lett.*, 2012, **100**, 021601.
28. P. Jacobson, B. Stoeger, A. Garhofer, G. S. Parkinson, M. Schmid, R. Caudillo, F. Mittendorfer, J. Redinger and U. Diebold, *J. Phys. Chem. Lett.*, 2012, **3**, 136.
29. P. Jacobson, B. Stoger, A. Garhofer, G. S. Parkinson, M. Schmid, R. Caudillo, F. Mittendorfer, J. Redinger and U. Diebold, *ACS Nano*, 2012, **6**, 3564.
30. J. Lahiri, T. Miller, L. Adamska, Oleynik, II and M. Batzill, *Nano Lett.*, 2011, **11**, 518.
31. J. Lahiri, T. S. Miller, A. J. Ross, L. Adamska, Oleynik, II and M. Batzill, *New J. Phys.*, 2011, **13**, 025001.
32. J. Sanchez-Barriga, A. Varykhalov, M. R. Scholz, O. Rader, D. Marchenko, A. Rybkin, A. M. Shikin and E. Vescovo, *Diam. Relat. Mat.*, 2010, **19**, 734.
33. T. Iwasaki, A. A. Zakharov, T. Eelbo, M. Waśniowska, R. Wiesendanger, J. H. Smet and U. Starke, *Surf. Sci.*, 2014, **625**, 44.
34. V. Coropceanu, J. Cornil, D. A. da Silva, Y. Olivier, R. Silbey and J. L. Bredas, *Chem. Rev.*, 2007, **107**, 926.
35. D. Usachov, M. Brzhezinskaya, A. M. Shikin and V. K. Adamchuk, *Fullerenes, Nanotubes and Carbon Nanostruct.*, 2010, **18**, 487.
36. J. A. Smerdon, M. Bode, N. P. Guisinger and J. R. Guest, *Phys. Rev. B*, 2011, **84**, 165436.
37. A. V. Talyzin, S. M. Luzan, K. Leifer, S. Akhtar, J. Fetzer, F. Cataldo, Y. O. Tsybin, C. W. Tai, A. Dzwilewski and E. Moons, *J. Phys. Chem. C*, 2011, **115**, 13207.
38. J. Cai, P. Ruffieux, R. Jaafar, M. Bieri, T. Braun, S. Blankenburg, M. Muoth, A. P. Seitsonen, M. Saleh, X. Feng, K. Muellen and R. Fasel, *Nature*, 2010, **466**, 470.
39. B. Hu, H. Ago, Y. Ito, K. Kawahara, M. Tsuji, E. Magome, K. Sumitani, N. Mizuta, K. Ikeda and S. Mizuno, *Carbon*, 2012, **50**, 57.
40. R. G. Musket, W. McLean, C. A. Colmenares, D. M. Makowiecki and W. J. Siekhaus, *Appl. Surf. Sci. (1977-1985)*, 1982, **10**, 143.
41. G. Katz, *Appl. Phys. Lett.*, 1968, **12**, 161.
42. K. M. Reddy, A. D. Gledhill, C.-H. Chen, J. M. Drexler and N. P. Padture, *Appl. Phys. Lett.*, 2011, **98**, 113117.
43. I. Horcas, R. Fernandez, J. M. Gomez-Rodriguez, J. Colchero, J. Gomez-Herrero and A. M. Baro, *Rev. Sc. Instrum.*, 2007, **78**, 013705.
44. N. Troullier and J. L. Martins, *Phys. Rev. B*, 1991, **43**, 1993.
45. T. Kosugi, T. Miyake, S. Ishibashi, R. Arita and H. Aoki, *Phys. Rev. B*, 2011, **84**, 020507.
46. P. Ordejon, E. Artacho and J. M. Soler, *Phys. Rev. B*, 1996, **53**, 10441.
47. J. M. Soler, E. Artacho, J. D. Gale, A. Garcia, J. Junquera, P. Ordejon and D. Sanchez-Portal, *J. Phys.:Condens. Matter*, 2002, **14**, 2745.
48. J. P. Perdew and A. Zunger, *Phys. Rev. B*, 1981, **23**, 5048.
49. J. R. Shewchuk, *An Introduction to the Conjugate Gradient Method Without the Agonizing Pain*, Carnegie Mellon University, 1994.
50. M. J. Frisch, G. W. Trucks, H. B. Schlegel, G. E. Scuseria, M. A. Robb, J. R. Cheeseman, G. Scalmani, V. Barone, B. Mennucci, G. A. Petersson, H. Nakatsuji, M. Caricato, X. Li, H. P. Hratchian, A. F. Izmaylov, J. Bloino, G. Zheng, J. L. Sonnenberg, M. Hada, M. Ehara, K. Toyota, R. Fukuda, J. Hasegawa, M. Ishida, T. Nakajima, Y. Honda, O. Kitao, H. Nakai, T. Vreven, J. A. Montgomery, J. E. Peralta, F. Ogliaro, M. Bearpark, J. J. Heyd, E. Brothers, K. N. Kudin, V. N. Staroverov, R. Kobayashi, J. Normand, K. Raghavachari, A. Rendell, J. C. Burant, S. S. Iyengar, J. Tomasi, M. Cossi, N. Rega, J. M. Millam, M. Klene, J. E. Knox, J. B. Cross, V. Bakken, C. Adamo, J. Jaramillo, R. Gomperts, R. E. Stratmann, O. Yazyev, A. J. Austin, R. Cammi, C. Pomelli, J. W. Ochterski, R. L. Martin, K. Morokuma, V. G. Zakrzewski, G. A. Voth, P. Salvador, J. J. Dannenberg, S. Dapprich, A. D. Daniels, Farkas, J. B. Foresman, J. V. Ortiz, J. Cioslowski and D. J. Fox, Wallingford CT, 2009.
51. M. D. Hanwell, D. E. Curtis, D. C. Lonie, T. Vandermeersch, E. Zurek and G. R. Hutchison, *J. Cheminf.*, 2012, **4**, 1.
52. Accelrys Software Inc., *Discovery Studio Modeling Environment, Release 4.0, San Diego: Accelrys Software Inc.*, 2013,
53. E. Voloshina and Y. Dedkov, *Phys. Chem. Chem. Phys.*, 2012, **14**, 13502.
54. W. Zhao, S. M. Kozlov, O. Hofert, K. Gotterbarm, M. P. A. Lorenz, F. Vines, C. Papp, A. Gorling and H. P. Steinruck, *J. Phys. Chem. Lett.*, 2011, **2**, 759.
55. M. Treier, C. A. Pignedoli, T. Laino, R. Rieger, K. Müllen, D. Passerone and R. Fasel, *Nat. Chem.*, 2011, **3**, 61.
56. D. Y. Zhong, J. H. Franke, S. K. Podiyanachari, T. Blomker, H. M. Zhang, G. Kehr, G. Erker, H. Fuchs and L. F. Chi, *Science*, 2011, **334**, 213.
57. A. Wiengarten, K. Seufert, W. Auwärter, D. Ecija, K. Diller, F. Allegretti, F. Bischoff, S. Fischer, D. A. Duncan, A. C.

Nanoscale Accepted Manuscript

 This journal is © The Royal Society of Chemistry 2012

Papageorgiou, F. Klappenberger, R. G. Acres, T. H. Ngo and J. V. Barth, *J. Am. Chem. Soc.*, 2014, **136**, 9346.
58. H.-Y. Gao, P. A. Held, M. Knor, C. Mück-Lichtenfeld, J. Neugebauer, A. Studer and H. Fuchs, *J. Am. Chem. Soc.*, 2014, **136**, 9658.
59. L. B. Roberson, J. Kowalik, L. M. Tolbert, C. Kloc, R. Zeis, X. L. Chi, R. Fleming and C. Wilkins, *J. Am. Chem. Soc.*, 2005, **127**,
60. Z. P. Liu and P. Hu, *J. Am. Chem. Soc.*, 2003, **125**, 1958.
61. J. K. Norskov, T. Bligaard, A. Logadottir, S. Bahn, L. B. Hansen, M. Bollinger, H. Bengaard, B. Hammer, Z. Sljivancanin, M. Mavrikakis, Y. Xu, S. Dahl and C. J. H. Jacobsen, *J. Catal.*, 2002, **209**, 275.
62. R. T. Vang, K. Honkala, S. Dahl, E. K. Vestergaard, J. Schnadt, E. Laegsgaard, B. S. Clausen, J. K. Norskov and F. Besenbacher, *Surf. Sci.*, 2006, **600**, 66.
63. L. L. Patera, C. Africh, R. S. Weatherup, R. Blume, S. Bhardwaj, C. Castellarin-Cudia, A. Knop-Gericke, R. Schloegl, G. Comelli, S. Hofmann and C. Cepek, *ACS Nano*, 2013, **7**, 7901.
64. A. C. Ferrari and D. M. Basko, *Nat. Nanotechnol.*, 2013, **8**, 235.
65. C. Busse, P. Lazic, R. Djemour, J. Coraux, T. Gerber, N. Atodiresei, V. Caciuc, R. Brako, A. T. N'Diaye, S. Blugel, J. Zegenhagen and T. Michely, *Phys. Rev. Lett.*, 2011, **107**, 036101.
66. L. Gao, *Graphene and 2D Materials*, 2014, **1**, 23.
67. Y. Murata, V. Petrova, B. B. Kappes, A. Ebnonnasir, I. Petrov, Y.-H. Xie, C. V. Ciobanu and S. Kodambaka, *ACS Nano*, 2010, **4**, 6509.
68. Y.-C. Chen, D. G. de Oteyza, Z. Pedramrazi, C. Chen, F. R. Fischer and M. F. Crommie, *ACS Nano*, 2013, **7**, 6123.
69. S. Kawai, B. Eren, L. Marot and E. Meyer, *ACS Nano*, 2014, **8**, 5932.
70. F. Varchon, P. Mallet, L. Magaud and J. Y. Veuillen, *Phys. Rev. B*, 2008, **77**, 165415.
71. L. Gao, J. R. Guest and N. P. Guisinger, *Nano Lett.*, 2010, **10**, 3512.
72. O. V. Yazyev and S. G. Louie, *Phys. Rev. B*, 2010, **81**, 195420.
73. N. Reckinger, E. Hooijdonk, F. Joucken, A. V. Tyurnina, S. Lucas and J.-F. Colomer, *Nano Res.*, 2014, **7**, 154.
74. D. L. Miller, M. W. Keller, J. M. Shaw, A. N. Chiaramonti and R. R. Keller, *J. Appl. Phys.*, 2012, **112**, 064317.

Nanoscale Accepted Manuscript